Monitoring the buildup of the quantum dot polaron: Pump-probe and four-wave mixing spectra from excitons and biexcitons in semiconductor quantum dots

A. Krügel,[1] A. Vagov,[2] V. M. Axt,[1] and T. Kuhn[1]
[1]*Institut für Festkörpertheorie, Westfälische Wilhelms-Universität Münster, Wilhelm-Klemm-Strasse 10, D-48149, Münster, Germany*
[2]*Physics Department, Lancaster University, Lancaster LA1 4YB, United Kingdom*
(Received 23 October 2006; revised manuscript received 3 May 2007; published 2 November 2007)

Pump-probe (PP) and four-wave mixing (FWM) signals from a single quantum dot are presented which are based on a four-level quantum dot model, accounting for the fine structure splitting as well as for the biexciton binding and phonon-induced pure dephasing. We have derived closed form analytical expressions for the PP and FWM polarization components in the time domain after excitation with a pair of ultrafast laser pulses. The solutions are exact within this model. We discuss the dependence of the signals on the polarization of the exciting pulses. We show that for PP spectra after excitation with collinearly polarized pulses and for FWM spectra after cocircular excitation changes in the line shape are entirely due to the polaron formation leading to a fixed shape when this process is completed. For PP spectra after cocircular excitation and FWM spectra after collinear excitation in general periodic modulations of the shape are superimposed which persist even on long time scales and reflect quantum beats due to the fine structure splitting or the biexciton binding energy.

DOI: 10.1103/PhysRevB.76.195302 PACS number(s): 78.67.Hc, 73.20.Mf, 63.22.+m, 63.20.Kr

I. INTRODUCTION

The concept of *quasiparticles* which incorporate parts of the collective interaction among particles is a fruitful concept in condensed matter physics to simplify the description of interacting many-body systems. Prominent examples are phonons, excitons, plasmons, or polarons. Under external excitation their constituents may rearrange to minimize their interaction energy which then leads to the formation of a new stable complex, a new quasiparticle. For ultrafast impulsive excitations this "dressing" of the "bare" particle states is not instantaneous. The buildup of the new quasiparticles or elementary excitations occurs on a characteristic time scale of the many-body interaction, reflecting memory effects that are caused by quantum coherences in the system.[1,2] Thus, monitoring the formation of such an elemantary excitation gives a deep insight into quantum mechanical many-particle interactions. A powerful tool for this purpose is ultrafast laser spectroscopy which has already been successfully employed to monitor the buildup of screening in GaAs.[3,4] There an initially excited bare electron gets "dressed" by the other electrons and holes which eventually results in the formation of a plasmon resonance.[5]

In this paper we will analyze another example, the formation of a quantum dot (QD) acoustic polaron after impulsive excitation. QDs are distinguished systems for studying fundamental quantum mechanics in solid state systems since they resemble *artificial atoms* due to their atomiclike energy structure. Furthermore QDs attract great interest because of versatile possibilities to use them in optical devices such as quantum dot lasers,[6] single-photon sources,[7] or potentially as *qubits* in quantum computers.[8–12] For these applications a good knowledge of the optical properties and also of the decoherence mechanisms is vital. Besides the characterization of photoluminescence and absorption, in particular, nonlinear optical signals are instructive, e.g., pump-probe[13,14] (PP) and four-wave mixing[15–18] (FWM) measurements. Among the various types of QDs self-assembled QDs resemble most closely the ideal of an artificial macroatom, due to a strong carrier confinement and a resulting large energy level separation. Because of the typically high density of dots in the grown samples and the small dipole moments, which lead only to weak optical signals, first experimental studies of self-assembled QDs have been made on ensembles of these nanostructures. Meanwhile improvement of the fabrication of QDs and of the detection techniques has made it possible to experimentally study linear and nonlinear optical signals from single self-assembled QDs.[19–29] Although PP signals from single interface QDs, due to their larger dipole moments, had already been obtained,[30–36] only most recently PP[37] and FWM[38] signals from single self-assembled QDs have been reported manifesting new progress in this field. Since QDs, unlike real atoms, are embedded in a solid state matrix they are more strongly exposed to influences from the environment that destroy quantum mechanical coherences. However, differently from higher dimensional semiconductor systems, where transitions mediated by the coupling to phonons are a major decoherence mechanism, these processes are strongly suppressed in QDs when the phonon energy does not match the electronic transition energy—an effect commonly called *phonon bottleneck*. As a consequence *pure dephasing* processes which do not change the electronic occupations become more important. Indeed pure dephasing processes due to the interaction with longitudinal acoustic (LA) phonons have been found to be the main cause for decoherence of the optical interband polarization on short time scales of about a few picoseconds in typical III-V QDs of small size, i.e., with large level separation.[28,39–42] Within these few picoseconds a polaron complex is built up, physically corresponding to a lattice distortion that minimizes the interaction energy between the phonons and the excited carrier pair. Theoretically pure dephasing processes are described by the *independent boson model*. Many studies have investigated the influence of pure dephasing on the optical properties of QDs, e.g., on the spectral shape of the linear absorption,[40] on Rabi oscillations[43–45] and on FWM signals[46] where quantitative agreement with experimental results has

been found.[42] In most of these works only the lowest exciton state of the QD has been taken into account. This is a good approximation for circularly polarized excitation of strongly confined QDs with nearly cylindrical symmetry, i.e., with large level spacing and vanishing fine structure splitting. Then only one spin-polarized exciton eigenstate is excited and the QD is effectively reduced to a two-level system. However, within that description the dependence of nonlinear optical signals on the polarization of the exciting pulses, observed, e.g., in time-integrated FWM experiments,[47] cannot be explained. We have recently extended the theory to a model where not only one exciton, but two orthogonally polarized bright exciton eigenstates and the biexciton state are included.[48] Thus, also effects of the fine structure splitting and the biexciton binding are taken into account. It is well known that the presence of biexcitons has a considerable influence on the optical properties of QDs.[49–51] With regard to device applications a thorough understanding of these properties is required, especially when biexcitons are the crucial part of the device, for instance, as sources for entangled or squeezed photons[52–54] or as quantum computing devices.[30–55]

In this paper we concentrate on the influence of phonon-induced pure dephasing on PP and FWM signals from single strongly confined QDs. We demonstrate that the line shape of phonon-induced background spectra in dependence on the delay time monitors the polaron dressing process. The calculation of the signals is based on the theory presented in Ref. 48. There a recursion formula for the exact analytical solution for all density matrix elements of the coupled QD-acoustic phonon system under excitation with an arbitrary series of ultrafast laser pulses has been provided. Here we derive closed form expressions for the case of two-pulse excitation either in a PP or in a FWM setup.

The paper is organized as follows: In Sec. II we specify our model. In Sec. III A we present results for PP signals after collinear as well as after cocircular excitation considering both *positive* and *negative delay* conditions. We give the analytical formulas and discuss the resulting phonon background spectra. Section III B is dedicated to the FWM signals after two-pulse excitation. We treat the same excitation conditions as for the PP case and give the respective analytical formulas and some of the corresponding spectra. The results are compared to the findings within the two-level model.[46] Section IV then summarizes our work and draws some conclusions.

II. THEORY

We consider a QD in the strong confinement limit modeled by an electronic four-level system coupled to phonons and to an external laser field. The four electronic eigenstates are the ground state of the unexcited dot, $|0\rangle$, the two linearly polarized single exciton states, $|x\rangle=(|\sigma^+\rangle+|\sigma^-\rangle)/\sqrt{2}$ and $|y\rangle=-i(|\sigma^+\rangle-|\sigma^-\rangle)/\sqrt{2}$, and the biexciton state, $|B\rangle=c^\dagger_{-1/2}d^\dagger_{3/2}c^\dagger_{1/2}d^\dagger_{-3/2}|0\rangle$. Here the angular momentum states are defined as $|\sigma^+\rangle=c^\dagger_{-1/2}d^\dagger_{3/2}|0\rangle$ and $|\sigma^-\rangle=c^\dagger_{1/2}d^\dagger_{-3/2}|0\rangle$, where $c^\dagger_\sigma$ $[d^\dagger_\sigma]$ denote the creation operator of an electron in the lowest conduction band state (a hole in the heavy hole band state) with angular momentum quantum number m^e_J $[m^h_J]$ indicated by the subscript. The single exciton states are split by the fine structure splitting $\hbar\Delta_{\mathrm{ex}}$ resulting from the long-range part of the electron-hole exchange interaction.[20] Here we have assumed that the exchange potential is independent of the spin polarization which implies that the linearly polarized exciton states may be written in the above mentioned superposition of the spin basis states. For the angular momentum states the usual selection rules imply that σ^+-polarized light couples the $m^h_J=+3/2$ hole to the $m^e_J=-1/2$ electron and σ^--polarized light couples the $m^h_J=-3/2$ hole to the $m^e_J=+1/2$ electron. Thus the optical interband polarization of the QD can be written in the electronic eigenbasis $|\nu\rangle=|0\rangle,|x\rangle,|y\rangle,|B\rangle$ as

$$\langle\hat{\mathbf{P}}\rangle=\frac{M_0^*}{\sqrt{2}}[(C_{0x}-iC_{0y}+C_{xB}-iC_{yB})\mathbf{e}_{\sigma^+}+(C_{0x}+iC_{0y}+C_{xB}+iC_{yB})\mathbf{e}_{\sigma^-}], \tag{1}$$

where M_0 denotes the dipole matrix element between valence and conduction band states and $\mathbf{e}_{\sigma^\pm}$ are the unit vectors along the $\sigma^\pm$ polarization components. $C_{\nu\nu'}=\langle|\nu\rangle\langle\nu'|\rangle$ denote the electronic coherences between the states $|\nu\rangle$ and $|\nu'\rangle$, which are given by the elements of the density matrix in the electronic eigenbasis. The linearly polarized components of the optical polarization are then obtained by transforming to the Cartesian unit vectors $\mathbf{e}_{x/y}$ according to $\mathbf{e}_{\sigma^\pm}=(\mathbf{e}_x\pm i\mathbf{e}_y)/\sqrt{2}$. We determine the density matrix elements with the help of generating functions. The general technique as well as its application to a four-level QD model are explained in detail in Ref. 48. Here we will present and discuss the results for nonlinear optical signals after excitation by two laser pulses.

To set up the equations of motion we have employed the Hamiltonian in the electronic eigenbasis

$$H=\sum_\nu\hbar\omega_\nu|\nu\rangle\langle\nu|-\sum_{\nu\nu'}\hbar\bar{M}_{\nu\nu'}|\nu\rangle\langle\nu'|+\sum_\xi\hbar\omega_\xi b^\dagger_\xi b_\xi+\sum_{\nu\xi}\hbar(g^\nu_\xi b_\xi+g^{\nu^*}_\xi b^\dagger_\xi)|\nu\rangle\langle\nu|, \tag{2}$$

where $\hbar\omega_\nu=\mathcal{E}_\nu$ is the energy of the eigenstate $|\nu\rangle$ (cf. the sketch of the energy scheme in Fig. 1). For the interaction with the phonon system we concentrate on pure dephasing processes as described by the *independent boson model*.[56] The coupling strength between the electronic state $|\nu\rangle$ and the phonon mode with energy $\hbar\omega_\xi$ is determined by the element g^ν_ξ. In our calculations we assume $g^\nu_\xi=(g^e_\xi-g^h_\xi)n_\nu$ with n_ν denoting the number of electron-hole pairs in the state, which holds for the strong confinement limit where correlations with higher electronic states can be neglected, and we consider for the coupling matrix elements of electrons and holes, $g^{e/h}_\xi$, the usual deformation potential coupling elements for carrier-LA-phonon interaction[42,43,46] where Gaussian wave functions for the carriers have been assumed. Since moderate changes in the geometry would not lead to a qualitative difference in the results,[57] we use the same carrier-phonon coupling elements also when nonvanishing exchange splitting is taken into account, although this is usually con-

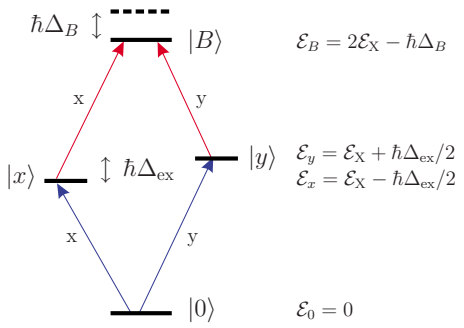

FIG. 1. (Color online) Sketch of the four-level system consisting of the ground state (unexcited QD), the two linearly polarized single exciton states, and the biexciton state.

nected with wave functions deviating from cylindrical symmetry. The same standard GaAs material parameters as in Ref. 44 have been employed and the localization length of the Gaussian electron wave function is chosen to be 4 nm.

The coupling of the excitons to an external laser field is described by the matrix

$$\bar{M} = \begin{pmatrix} 0 & \Omega_x^* & -\Omega_y^* & 0 \\ \Omega_x & 0 & 0 & \Omega_x^* \\ -\Omega_y & 0 & 0 & -\Omega_y^* \\ 0 & \Omega_x & -\Omega_y & 0 \end{pmatrix}, \tag{3}$$

with $\Omega_x = (\Omega_{\sigma^+} + \Omega_{\sigma^-})/\sqrt{2}$ and $\Omega_y = -i(\Omega_{\sigma^+} - \Omega_{\sigma^-})/\sqrt{2}$. The instantaneous Rabi frequencies $\Omega_{\sigma^\pm}$ for the dipole transitions from the ground state to the spin-polarized $|\sigma^\pm\rangle$ exciton state are given by

$$\Omega_{\sigma^\pm} = M_0 E_{\sigma^\pm}/\hbar = \sum_{j=1}^{2} \frac{f_{j\sigma^\pm}}{2} e^{i\phi_{j\sigma^\pm}} \delta(t - t_j), \tag{4}$$

where the summation refers to the two exciting pulses. We model the time dependence of the $\sigma^\pm$ component of the laser field amplitude, $E_{\sigma^\pm}$, by a δ function. This description holds in the limit of pulses shorter than the characteristic electron-phonon coupling time, which is typically about 1 ps. In the following the jth pulse arriving at time t_j will be characterized by its pulse area f_j and its phase ϕ_j. In the case of σ^+-[σ^--] circularly polarized excitation we have $f_j = f_{j\sigma^+}$ [$f_j = f_{j\sigma^-}$] and the respective phase $\phi_j = \phi_{j\sigma^+}$ [$\phi_j = \phi_{j\sigma^-}$]. For linear polarization we set $f_j = 2f_{j\sigma^+} = 2f_{j\sigma^-}$ with the corresponding phase $\phi_j = \phi_{j\sigma^+} = \phi_{j\sigma^-}$ for x-polarized light and $\phi_j = \phi_{j\sigma^+} = \phi_{j\sigma^-} + \pi$ for y-polarized light. These definitions of the pulse areas f_j ensure that both for circularly and linearly polarized excitation a π pulse results in maximally occupied single exciton states.

III. RESULTS

A. Pump-probe signals

PP signals provide information about the system's answer to a test (probe) pulse in dependence on a pump pulse. From the general two-pulse solution for the optical polarization in the time domain we have extracted the PP signals by collecting the contributions which are proportional to $\exp\{i\phi_t\}$, with ϕ_t being the phase of the test pulse. Since usually the test pulse is assumed to be weak, we have linearized the signals with respect to this pulse. As usual we refer to *positive delays* when the pump pulse, characterized by the pulse area f_p, precedes the test pulse with pulse area f_t.

Let us first concentrate on the excitation by two collinearly polarized pulses. To be specific x polarization has been chosen. Then, for positive delay the x component of the PP polarization reads

$$\langle \hat{P}_{xx}^{PP} \rangle_x = i \frac{M_0^*}{2\sqrt{2}} \theta(t) f_t \{ [\bar{C}_0^x K_0^E - \bar{C}_x^x K_x^E] e^{-i\omega_x t} + [\bar{C}_x^x K_x^B - \bar{C}_B^x K_B^B] e^{-i\omega_{Bx} t} \}, \tag{5}$$

where we have set the arrival time of the pump pulse to $t = -\tau$ and that of the probe pulse to $t = 0$. Here, as in the following formulas, we have omitted the phase factor $\exp\{i\phi_t\}$ that was used to identify the PP signal component. The signal consists of two parts corresponding to the ground state to exciton transition (GET) with frequency ω_x and the exciton to biexciton transition (EBT) with frequency $\omega_{Bx} = \omega_B - \omega_x$, respectively. The contributions are determined by the occupations of the electronic levels right after the pump pulse, $\bar{C}_\nu^x = \lim_{\varepsilon \to 0^+} C_{\nu\nu}(-\tau + \varepsilon)$, times a function K_ν^α. The occupations $\bar{C}_\nu^x$ depend only on the pulse area f_p as follows:

$$\bar{C}_0^x = \cos^4 \frac{f_p}{4}, \quad \bar{C}_x^x = \frac{1}{2} \sin^2 \frac{f_p}{2}, \quad \bar{C}_B^x = \sin^4 \frac{f_p}{4}. \tag{6}$$

The upper index x indicates that we are considering x linearly polarized excitation. The functions $K_\nu^\alpha = K_\nu^\alpha(t, \tau)$ depend on the real time t, on the delay time τ, and on the properties of the phonon system, i.e., the phonon energies $\hbar\omega_\xi$ and dimensionless electron-phonon coupling elements $\gamma_\xi = (g_\xi^e - g_\xi^h)/\omega_\xi$. The upper index α is E for the functions contributing to the GET or B for the functions contributing to the EBT. All functions K_ν^α have the structure $K_\nu^\alpha = \tilde{K}_\nu^\alpha e^{\Xi(t)}$ with

$$\Xi(t) = -\sum_\xi |\gamma_\xi|^2 (2N_\xi + 1)(1 - \cos \omega_\xi t), \tag{7}$$

N_ξ being the thermal phonon occupation number, and $\tilde{K}_\nu^\alpha$ are time-dependent phase factors given by

$$\tilde{K}_0^E(t, \tau) = \tilde{K}_0^E(t) = e^{-i\Sigma_\xi |\gamma_\xi|^2 \sin \omega_\xi t}, \tag{8a}$$

$$\tilde{K}_x^E(t, \tau) = e^{i\Sigma_\xi |\gamma_\xi|^2 [2 \sin \omega_\xi \tau + \sin \omega_\xi t - 2 \sin \omega_\xi (t+\tau)]}, \tag{8b}$$

$$\tilde{K}_x^B(t, \tau) = e^{i\Sigma_\xi |\gamma_\xi|^2 [2 \sin \omega_\xi \tau - \sin \omega_\xi t - 2 \sin \omega_\xi (t+\tau)]}, \tag{8c}$$

$$\tilde{K}_B^B(t, \tau) = e^{i\Sigma_\xi |\gamma_\xi|^2 [4 \sin \omega_\xi \tau + \sin \omega_\xi t - 4 \sin \omega_\xi (t+\tau)]}. \tag{8d}$$

For delay times longer than the typical carrier-phonon interaction time τ_p, which is of the order of 1 ps (see below), the sums over the τ-dependent oscillations in Eqs. (8a)–(8d) average to zero. Thus, the functions become independent of τ

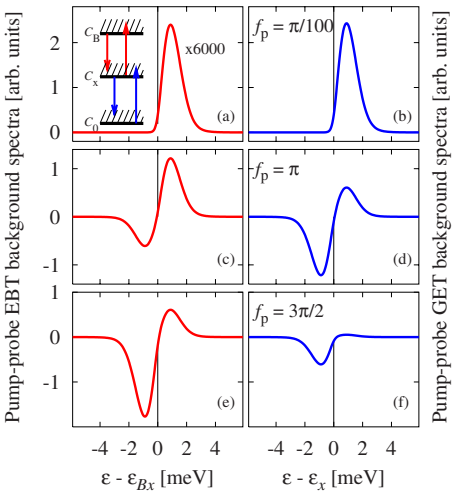

FIG. 2. (Color online) PP spectra for collinear (xx) excitation at long delay times and different pulse areas f_p of the pump pulse at low temperature ($T=1$ K).

with $\tilde{K}_0^E=\tilde{K}_x^B$ and $\tilde{K}_x^E=\tilde{K}_B^B$. Consequently, also the shape of the spectra does not change anymore. Physically this limit means that the lattice has reached its new equilibrium position when the second pulse arrives. In Fig. 2 we have plotted the phonon background spectra of the EBT and the GET for $\tau=4$ ps, i.e., a delay time which satisfies $\tau > \tau_p$, at temperature $T=1$ K for three different pump pulse areas. These PP spectra have been obtained as the imaginary part of the Fourier transform of Eq. (5). Since we do not include further decay mechanisms,[58–60] e.g., radiative decay, the long-time value of the polarization is nonzero, leading to unbroadened zero phonon lines (ZPLs). For the numerical calculation of the spectra we have eliminated the ZPLs by subtracting the final long-time value of the polarization for each transition. As a guide to the eye the ZPLs are indicated by vertical lines.

The physical origin of the spectra can be easily understood with the help of the three-level system sketched in the inset of Fig. 2(a) (since we consider only x linearly polarized pulses, the state $|y\rangle$ is never excited). Due to the carrier-phonon interaction each electronic state is accompanied by a phonon sideband, in the sketch indicated by the hatched areas. At low temperatures these sidebands are almost empty such that the probe pulse induces mainly transitions starting from the zero phonon state at the bottom of each sideband. Then, for excitation energies higher than the zero phonon transition energy the laser pulse can only generate transitions into the sideband of the energetically higher state while for excitation energies below the ZPL the transition has to end up in the phonon sideband of the energetically lower state. Thus at low temperature the spectra always exhibit gain on the left and absorption on the right hand side of the corresponding ZPL. This behavior may be nicely read off from the analytical formulas.

After a weak pump pulse with $f_p=\pi/100$ [Figs. 2(a) and 2(b)] the occupation of the ground state, $\bar{C}_x^0$, is still much stronger than the exciton occupation, $\bar{C}_x^x$, and the biexciton occupation, $\bar{C}_x^B$, is negligible. Thus we can see from the formula that the GET signal is essentially proportional to the ground state occupation and the EBT signal proportional to the single exciton occupation. The shape of the spectra agrees with the linear absorption spectrum[40] which is given by the Fourier transform of K_0^E. For zero temperature K_0^E is proportional to

$$K_0^E|_{T=0} \propto \exp\left\{\sum_\xi |\gamma_\xi|^2 e^{-i\omega_\xi t}\right\} \approx 1 + \sum_\xi |\gamma_\xi|^2 e^{-i\omega_\xi t},$$

where in the second form we have assumed that the lower exponential can be expanded in powers of the carrier-phonon coupling constant. This expansion up to second order is valid for not too strong carrier-phonon coupling. In particular, it is a good approximation for GaAs material parameters. It shows that in the low temperature limit the Fourier components are nonzero only for excitation frequencies higher than the zero phonon transitions which define the zero of the frequency scale. Thus in Figs. 2(a) and 2(b) only absorption but no gain is visible. Since because of the very small occupation of the single exciton state the EBT signal is much weaker than the GET signal, it has been multiplied by a factor of 6000.

For stronger pump pulses [Figs. 2(c)–2(f)] we have noticeable occupations of the exciton ($\bar{C}_x^x$) and biexciton ($\bar{C}_B^x$) states. In that case also the terms with K_x^E and K_B^B in Eq. (5) contribute noticeably to the spectra, however, with a negative sign indicating gain. For long delay times and $T=0$ K these phonon functions have the form

$$K_x^E|_{T=0} = K_B^B|_{T=0} \approx 1 + \sum_\xi |\gamma_\xi|^2 e^{i\omega_\xi t} \tag{9}$$

and lead to nonzero spectra on the left hand side of the ZPL. For a pulse area of the pump pulse $f_p=\pi$ [Figs. 2(c) and 2(d)] we have $\bar{C}_0^x=0.25$, $\bar{C}_x^x=0.5$, and $\bar{C}_B^x=0.25$ and we expect predominantly gain on the GET and absorption on the EBT, which is indeed observed. The ratio of the amplitudes of gain to absorption is determined by the occupations of the dressed states after the pump pulse, $\bar{C}_B^x:\bar{C}_x^x=0.25:0.5$ in Fig. 2(c) and $\bar{C}_x^x:\bar{C}_0^x=0.5:0.25$ in Fig. 2(d). Accordingly, for a pump pulse with $f_p=3\pi/2$ [Figs. 2(e) and 2(f)] with $\bar{C}_0^x=0.02$, $\bar{C}_x^x=0.25$, and $\bar{C}_B^x=0.73$ both transitions are strongly inverted and gain dominates in both cases.

For higher temperatures the phonon sidebands are considerably occupied up to an energy of about k_BT above the zero phonon state leading to transitions mediated by thermal phonons which result in absorption also for excitation energies lower and emission also for excitation energies higher than the zero phonon transition energy. For temperatures of about $T=20$ K or higher the signals become dominated by the thermal phonons, i.e., by the thermal occupation number N_ξ in Eq. (7), which is common to all K_ν^α. Thus the phase factors become irrelevant and the spectra become symmetric with respect to the ZPLs, as can be seen in Fig. 3, where we have plotted the same spectra as in Fig. 2 but for $T=77$ K. The sign of the spectra is determined by the occupations after the pump pulse, i.e., by the inversion of the respective transition. It is equal to that of the ZPL.

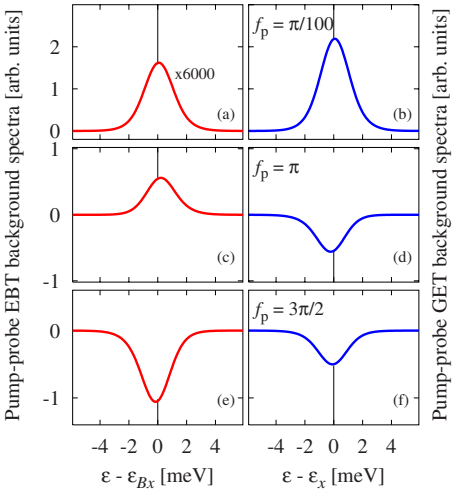

FIG. 3. (Color online) PP spectra for collinear (xx) excitation at long delay times and different pulse areas f_p of the pump pulse at elevated temperature (T=77 K).

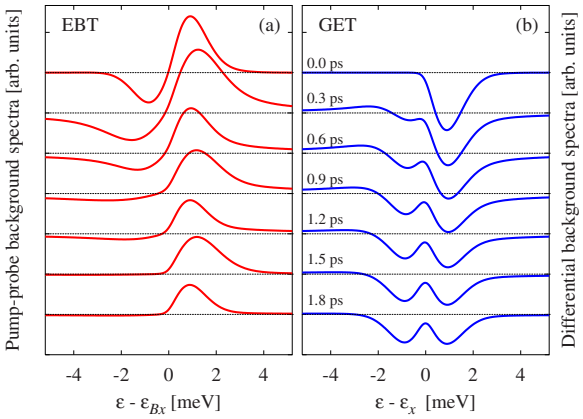

FIG. 4. (Color online) PP spectra for collinear (xx) excitation and different delay times at low temperature (T=1 K). (a) EBT; (b) GET differential signal (linear spectrum subtracted). The pump pulse area is $f_p = \pi/100$.

When the phase factors $\tilde{K}_\nu^\alpha$ become irrelevant obviously the dependence on τ in the PP polarization completely vanishes. Thus, at elevated temperatures the phonon spectra become independent of τ. For this reason in the following, when discussing the τ dependence of the PP spectra we will concentrate on low temperatures.

The spectra at long delay times could be well understood in terms of the occupations of the eigenstates of the coupled exciton-phonon system. It should be noted, however, that the excited zero phonon states in this picture are not the pure electronic eigenstates entering the Hamiltonian in Eq. (2), but they are dressed by the phonons and thus constitute polaronic states. The light field, on the other hand, directly couples to the pure electronic states. In the case of an ultrafast optical excitation initially these undressed states are populated. Then the phonon system reacts and the polaronic states build up within a characteristic electron-phonon interaction time, which depends on the phonon frequencies and the coupling matrix elements. This can be interpreted as the polaron dressing time τ_p. The buildup of the polaron in the region of the QD is associated with the emission of a phonon wave packet that carries away the energy which is released by the polaron formation.[61]

If τ is smaller than τ_p the spectral shape cannot be explained in terms of the occupations of the dressed states. In Fig. 4 we have plotted a series of spectra for EBT and GET with different delay times starting from τ=0 ps up to τ =1.8 ps. The pulse area of the pump pulse is $f_p = \pi/100$. Since in the case of such weak excitation the GET spectrum is strongly dominated by the linear spectrum of the unexcited QD, in Fig. 4(b) we have plotted the differential absorption spectrum obtained by subtracting the linear spectrum from the PP spectrum.

We observe a pronounced τ dependence of the spectra which reflects the polaron dressing process. For τ=0 ps the shape of the spectra is independent of the pulse area f_p, since the phonon system has not yet reacted to the pump pulse excitation. In that case the phonon functions for the respective transition coincide, $K_0^E(t,0) = K_x^E(t,0)$ and $K_x^B(t,0) = K_B^B(t,0)$, and thus can be taken out of the brackets in Eq. (5). This leaves the pulse-area dependent occupations as mere scaling factors which, however, can have either sign. With increasing τ the spectral shape changes until it reaches its final shape at a delay time of about $\tau \approx 1.5$ ps. Thus, for the present structural and material parameters this time can be interpreted as the polaron dressing time τ_p. During the buildup of the polaron the lattice is in a dynamic transition state when the probe pulse arrives which gives rise to a mixing of absorptive and dispersive features in the spectra resulting in a complex shape with long tails extending to energies quite far from the ZPL. (The zero level for each spectrum is indicated by a dotted horizontal line.) At $\tau > \tau_p$ the long-time limit discussed in Figs. 2(a) and 2(b) is reached.

Let us now turn to *negative delay time*, where the pump pulse arrives after the probe pulse. Here we use the convention that the probe pulse arrives at $t = -|\tau|$ and the pump pulse arrives at t=0. Then the PP polarization for collinear excitation reads

$$\langle \hat{P}_{xx}^{PP} \rangle_x^- = i \frac{M_0^*}{2\sqrt{2}} \theta(t + |\tau|) f_t \Bigg\{ K_0^E(t + |\tau|) e^{-i\omega_x(t+|\tau|)} \times \left[\theta(-t) + \theta(t) \cos \frac{f_p}{2} \cos^2 \frac{f_p}{4} \right] + K_B^-(t,\tau) e^{-i\omega_{Bx} t} \frac{\theta(t)}{2} \sin^2 \frac{f_p}{2} e^{-i\omega_x|\tau|} \Bigg\}, \quad (10)$$

with $K_B^-(t,\tau) = \tilde{K}_B^-(t,\tau) e^{\Xi(t+|\tau|)}$ and

$$\tilde{K}_B^-(t,\tau) = e^{-i\Sigma_\xi |\gamma_\xi|^2 [\sin \omega_\xi (t+|\tau|) + 2 \sin \omega_\xi t]}. \quad (11)$$

Again we have two contributions, one associated with the GET, which starts at the arrival time of the probe pulse and is modified when the pump pulse arrives, and the other associated with the EBT which only starts after the pump pulse has arrived. This is because the signal is linear with respect to the

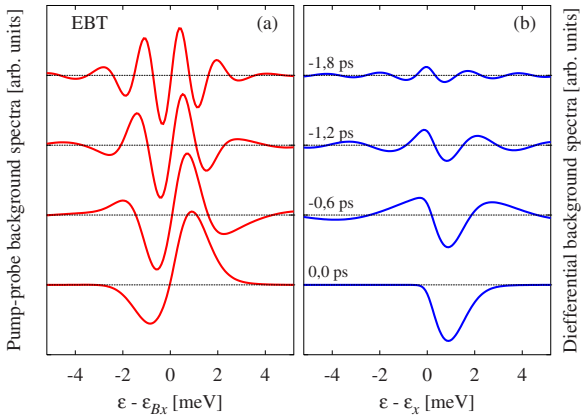

FIG. 5. (Color online) PP spectra for collinear (xx) excitation and different negative delay times at low temperature ($T=1$ K). (a) EBT; (b) GET differential signal. The pulse area is $f_p=\pi/100$.

probe pulse and in linear order the probe pulse alone cannot create an EBT signal.

Figure 5 shows the PP background spectra for weak x linearly polarized pump and probe pulses. For the GET we have plotted again the differential spectra. We observe that with increasing $|\tau|$ the spectra decrease and become superimposed with symmetric coherent spectral oscillations around the zero phonon transition. Such spectral oscillations appearing at negative delay times are a rather general feature and have been observed in many higher dimensional semiconductor systems[62–65] as well as in quantum dots created by interface fluctuations in thin quantum wells.[31] Their period is given by $2\pi\hbar/\tau$. The oscillations are caused by the instantaneous jump of the optical polarization at the arrival time of the pump pulse which reflects the perturbed free induction decay due to the nonlinear interaction of the pump pulse with the polarization excited by the preceding probe pulse. Here this nonlinear interaction leads to a jump in the GET polarization and the buildup of the EBT signal.

Let us conclude the discussion of the PP signals with some remarks about the cocircular excitation conditions. The mathematical structure of the signals is similar to the case of collinear excitation consisting of pulse-area dependent occupations and phonon functions. However, in general there are four contributions corresponding to the four possible transitions (cf. Fig. 1), two transitions from the ground state to the linearly polarized single exciton states and two transitions from these exciton states to the biexciton state. The explicit formulas both for positive and negative delays are given in the Appendix [Eqs. (A1) and (A2)]. Each transition consists of a ZPL and a phonon background. The distance between the ZPLs for the GETs and between the ZPLs for the EBTs is determined by the fine structure splitting $\hbar\Delta_{\mathrm{ex}}$. If in a QD this fine structure splitting vanishes the two single exciton states are degenerate. A circularly polarized excitation creates circularly polarized excitons which in this case are electronic eigenstates as well. Then, due to the selection rules the biexciton cannot be excited. The PP signal exhibits only a GET contribution which agrees with the result obtained for a two-level QD model.

Real QDs typically exhibit some finite exchange splitting. Then in general all four contributions are present in the PP

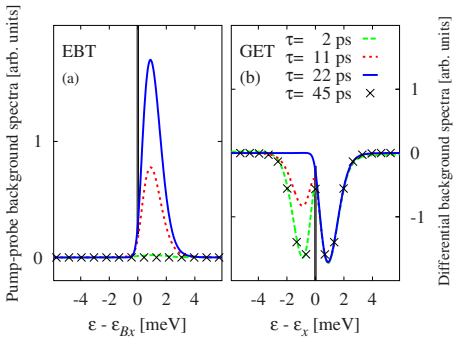

FIG. 6. (Color online) PP spectra for cocircular ($\sigma^+\sigma^+$) excitation and different delay times at low temperature ($T=1$ K). Note that both GET and EBT have two ZPLs separated by the fine structure splitting taken to be 90 μeV.

spectra. Even for cocircular excitation with σ^+ pulses the PP polarization has a σ^- component [cf. Eq. (A1)]. However, the fine structure splitting of the two GET ZPLs as well as of the two EBT ZPLs is usually less than about 150 μeV.[20,25,66] This energy difference is so small that the respective background spectra with an energy scale of a few meV practically coincide. This can be seen in Fig. 6 where the σ^+ components of differential GET and EBT background spectra are plotted with a fine structure splitting of 90 μeV for different values of τ. The ZPLs are indicated by vertical lines. On the energy scale of the figure their separation is hardly visible. All delay times chosen are longer than the polaron dressing time τ_p. Here we see a major difference compared to the collinear case. While there the spectra did not change anymore after the polaron formation, we now observe a pronounced time dependence on a much longer time scale. At the shortest time, $\tau=2$ ps, the differential GET signal is essentially symmetric and similar to the case of collinear excitation [cf. Fig. 4(b)]. However, an EBT signal does not appear. With increasing time an EBT signal builds up and the part below the ZPLs in the GET signal diminishes. The two contributions exhibit an oscillatory behavior with a period of about 44 ps.

The oscillations of the excitonic and biexcitonic contributions in the σ^+ component can be physically explained as follows. The σ^+-polarized pump pulse excites the spin-polarized exciton state $|\sigma^+\rangle$ which, for nonvanishing exchange coupling, is not an eigenstate but a linear combination of the two linearly polarized excitons. Thus it oscillates between the two spin polarizations with a frequency determined by the exchange splitting, and at the arrival of the second pulse the state of the system is described by the superposition

$$|\Psi(\tau)\rangle \propto \cos\left(\frac{\Delta_{\mathrm{ex}}\tau}{2}\right)|\sigma^+\rangle + i\sin\left(\frac{\Delta_{\mathrm{ex}}\tau}{2}\right)|\sigma^-\rangle. \qquad (12)$$

For short delay times or τ of about an oscillation period the system is almost in a pure $|\sigma^+\rangle$ state. Then, due to the Pauli blocking, the second σ^+-polarized pulse cannot excite the biexciton. Thus in Fig. 6 for $\tau=2$ ps and $\tau=45$ ps there is no EBT signal and the GET background spectra show absorp-

tion on the right and gain on the left hand side of the ZPLs. If the second pulse, however, comes after half an oscillation period, the system is in the $|\sigma^-\rangle$ state and the second pulse yields a maximum biexciton contribution manifested in absorption on the right hand side of the EBT's ZPLs. This corresponds to vanishing gain in the GET spectrum.

Indeed, from Eq. (A1) it can be seen that the contributions which are responsible for the low-energy part of the GET signal ($\propto K_x^E$) and for the EBT signal ($\propto K_x^B$) involve oscillatory factors as a function of τ with an oscillation period $2\pi/\Delta_{\text{ex}}$ determined by the fine structure splitting. For the σ^+-detection component, which is the relevant one for PP detection, the contributions from the two fine structure split transitions essentially add up.

B. Four-wave mixing signals

The two-pulse FWM signal corresponds to those parts of our analytical solution that are proportional to $\exp\{i(2\phi_2 - \phi_1)\}$. In higher dimensional systems FWM signals are given by the radiation from the sample into the $2\mathbf{k}_2 - \mathbf{k}_1$ direction, where $\mathbf{k}_1$ and $\mathbf{k}_2$ are the wave vectors of the pulses. For quantum dots, which radiate equally in all directions, the FWM signal may be detected with the help of phase modulations.[38,67] We speak of *positive delay* when the pulse with phase ϕ_2 arrives second. A detailed theoretical analysis of FWM signals from single QDs and QD ensembles within the two-level model has been published in Ref. 46 examining positive delay conditions, because within the two-level system there is no FWM signal for negative delay. In that work it was found that for low temperature the spectra, generally and independently of the details of the carrier-phonon coupling, evolve from an asymmetric shape for vanishing delay between the pulses to a symmetric one for delay times longer than the characteristic carrier-phonon interaction time τ_p. Within the present four-level QD model we obtain the following analytical formula for the x component of the FWM polarization in the time domain for positive delay and collinear (xx) excitation:

$$\begin{aligned}\langle \hat{P}_{xx}^{FWM}\rangle_x = &- iM_0^*\theta(t)\{[\tilde{D}_1^x\tilde{C}_{x0}^x G_{x0}^E(t,\tau)e^{i\omega_x\tau} \\ &- \tilde{D}_2^x\tilde{C}_{Bx}^x G_{Bx}^E(t,\tau)e^{i\omega_{Bx}\tau}]e^{-i\omega_x t} - [\tilde{D}_2^x\tilde{C}_{x0}^x G_{x0}^B(t,\tau)e^{i\omega_x\tau} \\ &- \tilde{D}_1^x\tilde{C}_{Bx}^x G_{Bx}^B(t,\tau)e^{i\omega_{Bx}\tau}]e^{-i\omega_{Bx}t}\}, \end{aligned} \tag{13}$$

where again the identifying phase factor, here $\exp\{i(2\phi_2 - \phi_1)\}$, has been omitted. The structure of the signal is similar to that for the PP polarization in Eq. (5). The terms proportional to $\exp\{-i\omega_x t\}$ and $\exp\{-i\omega_{Bx}t\}$ correspond to the GET and EBT, respectively. The dependence on the pulse areas is contained in the coefficients

$$\tilde{C}_{x0}^x = \sin(f_1/2)\cos^2(f_1/4)/\sqrt{2}, \tag{14a}$$

$$\tilde{C}_{Bx}^x = \sin(f_1/2)\sin^2(f_1/4)/\sqrt{2}, \tag{14b}$$

$$\tilde{D}_1^x = \sin^2(f_2/2)/2, \tag{14c}$$

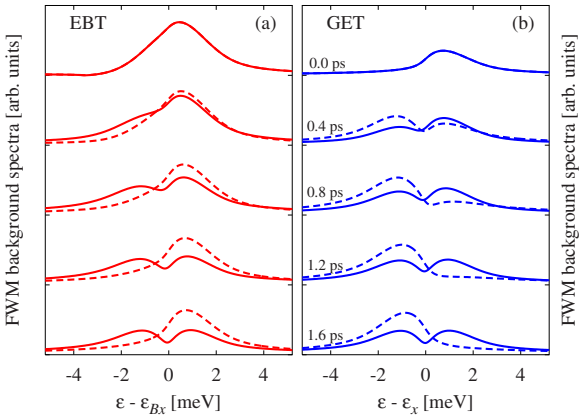

FIG. 7. (Color online) FWM spectra for collinear (xx) excitation and different delay times at low temperature ($T=1$ K). (a) EBT; (b) GET. The pulse areas are $f_1=f_2=\pi$ (solid lines) and $f_1=\pi$, $f_2=2\pi$ (dashed lines).

$$\tilde{D}_2^x = \cos(f_2/2)\sin^2(f_2/4). \tag{14d}$$

The coefficients $\tilde{C}_{\nu\nu'}^x$ are determined by the moduli of the off-diagonal elements of the density matrix of the system, $C_{\nu\nu'}$, right after the arrival of the first pulse. The upper index x again refers to x linearly polarized excitation. The functions $G_{\nu\nu'}^\alpha(t,\tau)$ depend on the real time, on the delay time, and on the properties of the phonon system, similar to the functions K_ν^α in the PP signal. They have also the structure $G_{\nu\nu'}^\alpha = \tilde{G}_{\nu\nu'}^\alpha e^{\Phi(t,\tau)}$ with

$$\begin{aligned}\Phi(t,\tau) = &- \sum_\xi |\gamma_\xi|^2(2N_\xi+1)[3 - 2\cos\omega_\xi t - 2\cos\omega_\xi\tau \\ &+ \cos\omega_\xi(t+\tau)]\end{aligned} \tag{15}$$

and time-dependent phase factors

$$\tilde{G}_{x0}^E(t,\tau) = e^{i\Sigma_\xi|\gamma_\xi|^2[2\sin\omega_\xi\tau - \sin\omega_\xi(t+\tau)]}, \tag{16a}$$

$$\tilde{G}_{Bx}^E(t,\tau) = e^{i\Sigma_\xi|\gamma_\xi|^2[6\sin\omega_\xi\tau + 2\sin\omega_\xi t - 3\sin\omega_\xi(t+\tau)]}, \tag{16b}$$

$$\tilde{G}_{x0}^B(t,\tau) = e^{i\Sigma_\xi|\gamma_\xi|^2[2\sin\omega_\xi\tau - 2\sin\omega_\xi t - \sin\omega_\xi(t+\tau)]}, \tag{16c}$$

$$\tilde{G}_{Bx}^B(t,\tau) = e^{i\Sigma_\xi|\gamma_\xi|^2[6\sin\omega_\xi\tau - 3\sin\omega_\xi(t+\tau)]}. \tag{16d}$$

As in the PP case here the phonon functions for the GET as well as those for the EBT coincide for zero delay, $G_{x0}^E(t,0) = G_{Bx}^E(t,0)$ and $G_{x0}^B(t,0) = G_{Bx}^B(t,0)$, such that the spectral shape of the FWM signal is independent of the pulse area for $\tau=0$ ps, provided that there is no spectral overlap between GET and EBT.

Figure 7 shows a series of EBT (a) and GET (b) background spectra for low temperature and different delay times. Note that since the FWM signal is in a background-free direction here the spectrum is given by the absolute value of the Fourier transform of the polarization. Solid and dashed lines refer to different choices of the pulse areas. The solid lines show the results for $f_1=f_2=\pi$. The choice of $f_1=\pi$

assures that the coefficients $\tilde{C}^x_{0x}$ and $\tilde{C}^x_{xB}$ are both nonzero; $f_2=\pi$ yields $\tilde{D}^x_2=0$. Thus only one term in Eq. (13) contributes to the GET, which in that case equals the solution for the two-level model.[46] Also one contribution to the EBT vanishes. The spectra for the EBT in the left panel and the GET in the right panel have different shapes at $\tau=0$ ps. Then the spectral shape changes with τ until for $\tau > \tau_p$ it becomes fixed and symmetric around the position of the respective ZPL, in agreement with what has been found previously for the GET within the two-level model. In the calculations of the spectra plotted with dashed lines we have kept the first pulse area $f_1=\pi$ but set $f_2=2\pi$. In that case we have $\tilde{D}^x_1=0$ and again two of the four terms in Eq. (13) vanish. Starting with the same spectral shapes as before GET and EBT evolve with increasing τ into asymmetric shapes, in qualitative difference to the previous case and also to the result for the two-level model, where at long delay times the spectra are necessarily symmetric. However, for both choices of the pulse area the spectral shapes of the GET and EBT are mirror symmetric for long delay times. This is a general result valid for arbitrary pulse areas, as can be seen from the long delay-time behavior of the phonon functions

$$G^E_{x0} = G^B_{Bx} \propto \exp\left\{\sum_\xi |\gamma_\xi|^2 (e^{i\omega_\xi t} + e^{-i\omega_\xi t})\right\}, \tag{17a}$$

$$G^E_{Bx} \propto \exp\left\{\sum_\xi |\gamma_\xi|^2 e^{i\omega_\xi t}\right\}, \tag{17b}$$

$$G^B_{x0} \propto \exp\left\{\sum_\xi |\gamma_\xi|^2 e^{-i\omega_\xi t}\right\}. \tag{17c}$$

In both cases the spectral shape for GET and EBT becomes fixed for long delay times. Note, however, that according to Eqs. (14a)–(14d) vanishing coefficients represent a special case and that generally there are two nonzero contributions to both GET and EBT in Eq. (13). These two contributions have different dependencies on τ, one oscillating with the frequency ω_x and the other with ω_{Bx}. Thus the FWM spectra exhibit an oscillatory τ dependence of the spectral shape with a periodicity determined by the biexciton binding frequency $\Delta_B \approx \omega_x - \omega_{Bx}$. Although the Fourier transform of each of the phonon functions does not change anymore with τ, the weight of their contribution does. This can be seen in Fig. 8, where we have plotted the GET spectra at four different delay times from 6.8 ps up to 8.0 ps for pulse areas of $f_1=\pi$ and $f_2=\pi/2$ [Fig. 8(a)] or $f_1=\pi$ and $f_2=3\pi/2$ [Fig. 8(b)]. The oscillation period is $T_B=2\pi/\Delta_B \approx 1.25$ ps. Obviously, the first and the last spectra with a delay difference of 1.2 ps almost coincide while in between the shape differs significantly. So, in contrast to the PP signals after collinear excitation, which acquire a fixed final shape for long delay times, we find for the same excitation conditions in the FWM signal changes of the spectral shape due to the biexciton binding even for delay times much longer than the time τ_p needed to build up the phonon dressed state.

For negative delay the analytical formula for the x component of the signal after collinear excitation is given in the Appendix [Eq. (A3)]. The signal is built up from the biexci-

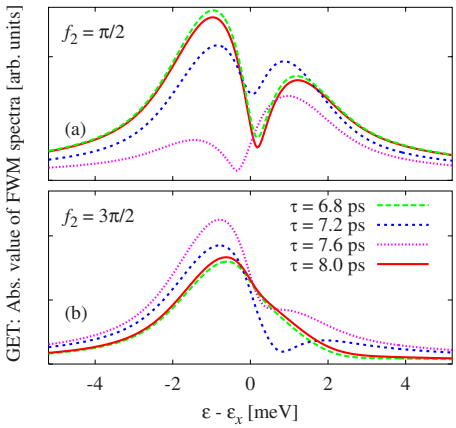

FIG. 8. (Color online) FWM spectra for collinear (xx) excitation and four different long delay times within an oscillation period of the biexciton binding energy. (a) GET for $f_1=\pi$ and $f_2=\pi/2$; (b) GET for $f_1=\pi$ and $f_2=3\pi/2$. The respective EBT spectra are mirror symmetric.

tonic coherence created by the first pulse, as can be seen from the factor $\exp\{-i\omega_B|\tau|\}$ in Eq. (A3). There are no spectral oscillations since there is no FWM signal before the arrival of the second pulse and the modulus of the Fourier transform does not depend on the time zero point chosen. Again the spectra of the GET and the EBT are mirror symmetric. Since they do not exhibit any pronounced feature which is different from the spectra already discussed we do not show a figure.

Finally, let us comment on the FWM signal after cocircular excitation with two σ^+ pulses, considering both the σ^+ as well as the σ^- component. The formulas are given in the Appendix [Eq. (A4)]. For QDs with zero exchange coupling where $\omega_x=\omega_y$, the σ^- component vanishes, leaving only the σ^+ component nonzero. The result then exactly coincides with that for the two-level model. However, even for nonvanishing fine structure splitting there is no biexciton contribution in the FWM signal, in contrast to the case of PP signals. The reason is that here the second pulse creates the transient grating from which it is diffracted. The grating is formed by the interference of the polarization created by the first pulse with the electric field of the second pulse. Thus, only the σ^+ component of the polarization of the first pulse can contribute to the grating which also explains why at delay times given by half integer multiples of the fine structure beat period, when the QD exciton created by the first pulse is in a $|\sigma^-\rangle$ state [cf. Eq. (12)], there is no FWM signal at all. As a function of τ the FWM signal oscillates with the fine structure beat period. The polarizations in Eq. (A4) contain only a single phonon function as a common factor. Thus, in contrast to the FWM signals after collinear excitation, but similar to the PP signals after collinear excitation, there are no changes of the shape of the phonon background for delay times longer than τ_p. The σ^+ and σ^- components of the FWM polarization only differ by the sign in front of the $|y\rangle$-exciton contribution. As a consequence, in the time domain the σ^--polarization component builds up only after about half a fine structure beat period. In the spectral domain two ZPLs

separated by the fine structure splitting can be found. The phonon background which has typically a much broader energy scale (cf. Fig. 6) almost cancels in the σ^- component of the spectrum whereas it adds up in the σ^+ component. The reduced background in the σ^- component can be ascribed to the extremely slow rise of the signal on the time scale of the fine structure period, which is therefore close to the adiabatic regime. Because of the small value of the fine structure splitting in real QDs the deviations from the behavior of a two-level system are very small explaining the excellent agreement of measured FWM signals for cocircular excitation with theoretical results obtained for a two-level QD model,[42] in particular, at times shorter than the fine structure beat period. Since a circularly polarized pulse cannot create a biexcitonic coherence, there is no FWM signal for cocircular excitation at *negative* τ, at least within our limit of ultrafast pulses. This is again in agreement with the behavior of a two-level model. Because of the similarity with the extensively discussed two-level results,[46] we do not show FWM spectra for the cocircular case.

IV. SUMMARY AND CONCLUSIONS

We have presented a detailed analysis of PP and FWM signals from single strongly confined quantum dots. Taking into account the two angular momentum states of electrons and holes the QD was described by a four-level model. In contrast to the previously treated two-level model this has allowed us to address the polarization dependence of the nonlinear optical signals.

PP signals after collinear excitation at long delay times could be well understood in terms of transitions between polaron dressed states. Due to the finite response time of the lattice, however, a finite time is required to build up these polaron states after an ultrafast optical excitation. At low temperature this polaron dressing process is directly reflected in the delay time dependence of PP signals which after the completion of the polaron dressing become independent of the delay time.

For cocircularly polarized pulses, on the other hand, the scenario strongly depends on the fine structure splitting. For a vanishing splitting the system is effectively reduced to a two-level system. Otherwise the pump pulse creates a superposition of the linearly polarized single exciton states giving rise to quantum beats. As a result, the PP spectra still exhibit a time dependence even after the buildup of the polaron due to contributions oscillating between excitonic gain and biexcitonic absorption.

The general characteristics of FWM signals are similar to PP signals. On the time scale of the polaron dressing process the spectral shape changes as in the PP case. When looking at the details, however, we find pronounced differences between PP and FWM signals and even sometimes a complementary behavior. In general the FWM spectra after collinear excitation exhibit an oscillatory delay time dependence of their shape with an oscillation period given by the biexciton binding energy. These periodic changes in the phonon-induced background spectra last on even after the polaron dressing process. For cocircular excitation, on the other hand, the spectral shape is constant for delay times longer than the duration of the polaron dressing. Only the magnitude oscillates with the fine structure beat period which is typically much longer than the electron-phonon interaction time. In contrast to PP signals, in FWM signals after cocircular excitation we never find a biexcitonic contribution even when the fine structure splitting is finite.

In this paper we have restricted ourselves to nonlinear optical signals of a single QD. Of course, signals obtained from an inhomogeneously broadened ensemble of such QDs can easily be constructed from our results. Indeed, such calculations well reproduce the measured time-integrated FWM signals both for collinear and cocircular excitation conditions,[47] in particular, the presence of biexciton quantum beats for collinear excitation and fine structure quantum beats for cocircular excitation.[68] Experimental results for PP or FWM signals from single QDs to date have mainly been reported for weakly confined QDs resulting from interface fluctuations,[30–36] where typically other dephasing mechanisms than pure dephasing are dominant. With such measurements performed on strongly confined QDs one should be able to directly monitor the buildup of a quantum mechanical quasiparticle, the polaron, involving both electronic and lattice degrees of freedom.

ACKNOWLEDGMENT

This work has been supported by the Deutsche Forschungsgemeinschaft (Grant No. Ku 697/9-2).

APPENDIX

In this appendix we summarize the results for the PP and FWM signals which have not been explicitly given above. The PP polarization after cocircular ($\sigma^+\sigma^+$) excitation for positive delay reads

$$\begin{aligned}\langle \hat{P}^{PP}_{++}\rangle_{\pm} = \frac{iM_0^* f_t}{4}\theta(t)\{e^{-i\omega_x t}[\bar{C}_0^+ K_0^E(t,\tau) - \bar{C}_x^+ K_x^E(t,\tau)\\ \times(1+e^{i\Delta_{\rm ex}\tau})] \pm e^{-i\omega_y t}[\bar{C}_0^+ K_0^E(t,\tau)\\ - \bar{C}_y^+ K_x^E(t,\tau)(1+e^{-i\Delta_{\rm ex}\tau})] + e^{-i\omega_{Bx}t}\bar{C}_x^+ K_x^B(t,\tau)\\ \times(1-e^{-i\Delta_{\rm ex}\tau}) \pm e^{-i\omega_{By}t}\bar{C}_y^+ K_x^B(t,\tau)(1-e^{i\Delta_{\rm ex}\tau})\}.\end{aligned} \tag{A1}$$

For negative delay we obtain

$$\begin{aligned}\langle \hat{P}^{PP}_{++}\rangle^-_{\pm} = i\frac{M_0^*}{4}\theta(t+|\tau|)f_t\{K_0^E(t+|\tau|)(e^{-i\omega_x(t+|\tau|)} \pm e^{-i\omega_y(t+|\tau|)})\\ \times[\theta(-t)+\theta(t)\bar{C}_0^+] + \theta(t)K_B^-(t,\tau)(\bar{C}_x^+ e^{-i\omega_{Bx}t}\\ \mp \bar{C}_y^+ e^{-i\omega_{By}t})(1-e^{-i\Delta_{\rm ex}|\tau|})e^{-i\omega_x|\tau|}\},\end{aligned} \tag{A2}$$

with K_ν^α and K_B^- defined in Eqs. (8) and (11). Here the upper sign refers to the σ^+ component and the lower sign to the σ^- component of the signal. The signals are mainly determined by the occupations of the electronic levels after the pump

pulse, which depend only on its pulse area f_p according to $\bar{C}_0^+ = \cos^2(f_p/2)$ and $\bar{C}_x^+ = \bar{C}_y^+ = \frac{1}{2}\sin^2(f_p/2)$.

The FWM polarization for collinear excitation at negative delay conditions, i.e., when the pulse with phase ϕ_2 precedes the pulse with phase ϕ_1, is given by

$$\langle \hat{P}_{xx}^{FWM} \rangle_x^- = -i\frac{M_0^*}{4\sqrt{2}}\theta(t)\sin^2\frac{f_2}{2}\sin\frac{f_1}{2}\cos^2\frac{f_1}{4}e^{-i\omega_B|\tau|} \times \{e^{-i\omega_x t}G_E^-(t,\tau) - e^{-i\omega_{Bx}t}G_B^-(t,\tau)\} \tag{A3}$$

with $G_\alpha^- = \tilde{G}_\alpha^- e^{\Phi^-(t,\tau)}$ and

$$\tilde{G}_E^-(t,\tau) = e^{-i\Sigma_\xi|\gamma_\xi|^2[2\sin\omega_\xi(t+|\tau|)+2\sin\omega_\xi|\tau|-\sin\omega_\xi t]},$$

$$\tilde{G}_B^-(t,\tau) = e^{-i\Sigma_\xi|\gamma_\xi|^2[2\sin\omega_\xi(t+|\tau|)+2\sin\omega_\xi|\tau|+\sin\omega_\xi t]},$$

$$\Phi^-(t,\tau) = -\sum_\xi |\gamma_\xi|^2(2N_\xi+1)[3-2\cos\omega_\xi(t+|\tau|) - 2\cos\omega_\xi|\tau| + \cos\omega_\xi t].$$

The $\sigma^\pm$ component of the polarization after cocircular excitation reads for positive delay

$$\langle \hat{P}_{++}^{FWM} \rangle_\pm = -i\frac{M_0^*}{\sqrt{2}}\theta(t)(e^{-i\omega_x t} \pm e^{-i\omega_y t})\tilde{D}^+\tilde{C}_{x0}^+ G_{x0}^E(t,\tau) \times (e^{i\omega_x\tau} + e^{i\omega_y\tau}), \tag{A4}$$

where the pulse area dependent coefficients are $\tilde{C}_{x0}^+ = \frac{1}{2\sqrt{2}}\sin(f_1)$ and $\tilde{D}^+ = \frac{1}{2}\sin^2(f_2/2)$.

For negative delay conditions, i.e., when the pulse with phase ϕ_2 precedes the pulse with phase ϕ_1, there is no FWM polarization after cocircular excitation, at least in our limit of ultrashort pulses.

[1] H. Haug and A. P. Jauho, *Quantum Kinetics for Transport and Optics in Semiconductors*, Series in Solid-State Sciences Vol. 123 (Springer, Berlin, 1996).
[2] V. Axt and T. Kuhn, Rep. Prog. Phys. **67**, 433 (2004).
[3] H. Haug, Nature (London) **414**, 261 (2001).
[4] R. Huber, F. Tauser, A. Brodschelm, M. Bichler, G. Abstreiter, and A. Leitenstorfer, Nature (London) **414**, 286 (2001).
[5] T. Wolterink, V. Axt, and T. Kuhn, Physica B **314**, 132 (2002).
[6] D. Bimberg, M. Grundmann, and N. N. Ledentsov, *Quantum Dot Heterostructures* (Wiley, Chichester, 1998).
[7] P. Michler, A. Kiraz, C. Becher, W. V. Schoenfeld, P. Petroff, L. D. Zhang, E. Hu, and A. Imamoglu, Science **290**, 2282 (2000).
[8] D. Loss and D. P. DiVincenzo, Phys. Rev. A **57**, 120 (1998).
[9] E. Biolatti, R. C. Iotti, P. Zanardi, and F. Rossi, Phys. Rev. Lett. **85**, 5647 (2000).
[10] A. Imamoglu, D. D. Awschalom, G. Burkard, D. P. DiVincenzo, D. Loss, M. Sherwin, and A. Small, Phys. Rev. Lett. **83**, 4204 (1999).
[11] G. Chen, T. H. Stievater, E. T. Batteh, X. Li, D. G. Steel, D. Gammon, D. S. Katzer, D. Park, and L. J. Sham, Phys. Rev. Lett. **88**, 117901 (2002).
[12] P. Zanardi and F. Rossi, Phys. Rev. Lett. **81**, 4752 (1998).
[13] P. Borri, W. Langbein, S. Schneider, U. Woggon, R. L. Sellin, D. Ouyang, and D. Bimberg, Phys. Rev. B **66**, 081306(R) (2002).
[14] H. Gotoh, H. Kamada, H. Nakano, T. Saitoh, H. Ando, and J. Temmyo, Appl. Phys. Lett. **87**, 102101 (2005).
[15] F. Gindele, U. Woggon, W. Langbein, J. M. Hvam, K. Leonardi, D. Hommel, and H. Selke, Phys. Rev. B **60**, 8773 (1999).
[16] H. P. Wagner, H.-P. Tranitz, H. Preis, W. Langbein, K. Leosson, and J. M. Hvam, Phys. Rev. B **60**, 10640 (1999).
[17] P. Borri, W. Langbein, S. Schneider, U. Woggon, R. L. Sellin, D. Ouyang, and D. Bimberg, Phys. Rev. Lett. **87**, 157401 (2001).
[18] D. Birkedal, K. Leosson, and J. M. Hvam, Phys. Rev. Lett. **87**, 227401 (2001).
[19] M. Bayer, A. Kuther, A. Forchel, A. Gorbunov, V. B. Timofeev, F. Schäfer, J. P. Reithmaier, T. L. Reinecke, and S. N. Walck, Phys. Rev. Lett. **82**, 1748 (1999).
[20] M. Bayer *et al.*, Phys. Rev. B **65**, 195315 (2002).
[21] K. Brunner, G. Abstreiter, G. Böhm, G. Tränkle, and G. Weimann, Phys. Rev. Lett. **73**, 1138 (1994).
[22] E. Dekel, D. Gershoni, E. Ehrenfreund, D. Spektor, J. M. Garcia, and P. M. Petroff, Phys. Rev. Lett. **80**, 4991 (1998).
[23] M. Grundmann *et al.*, Phys. Rev. Lett. **74**, 4043 (1995).
[24] A. Kuther, M. Bayer, A. Forchel, A. Gorbunov, V. B. Timofeev, F. Schäfer, and J. P. Reithmaier, Phys. Rev. B **58**, R7508 (1998).
[25] A. S. Lenihan, M. V. Gurudev Dutt, D. G. Steel, S. Ghosh, and P. K. Bhattacharya, Phys. Rev. Lett. **88**, 223601 (2002).
[26] R. Leon, P. M. Petroff, D. Leonard, and S. Fafard, Science **267**, 1966 (1995).
[27] J. Y. Marzin, J. M. Gérard, A. Izraël, D. Barrier, and G. Bastard, Phys. Rev. Lett. **73**, 716 (1994).
[28] T. Matsumoto, M. Ohtsu, K. Matsuda, T. Saiki, H. Saito, and K. Nishi, Appl. Phys. Lett. **75**, 3246 (1999).
[29] A. Zrenner, E. Beham, S. Stufler, F. Findeis, M. Bichler, and G. Abstreiter, Nature (London) **418**, 612 (2002).
[30] X. Li, Y. Wu, X. Xu, D. G. Steel, and D. Gammon, Phys. Rev. B **73**, 153304 (2006).
[31] T. Guenther, C. Lienau, T. Elsaesser, M. Glanemann, V. M. Axt, T. Kuhn, S. Eshlaghi, and A. D. Wieck, Phys. Rev. Lett. **89**, 057401 (2002).
[32] T. H. Stievater, X. Li, D. G. Steel, D. Gammon, D. S. Katzer, D. Park, C. Piermarocchi, and L. J. Sham, Phys. Rev. Lett. **87**, 133603 (2001).
[33] N. H. Bonadeo, G. Chen, D. Gammon, D. S. Katzer, D. Park, and D. G. Steel, Phys. Rev. Lett. **81**, 2759 (1998).
[34] J. Guest, T. Stievater, G. Chen, E. Tabak, B. Orr, D. Steel, D. Gammon, and D. Katzer, Science **293**, 2224 (2001).
[35] T. Unold, K. Mueller, C. Lienau, T. Elsaesser, and A. D. Wieck, Phys. Rev. Lett. **92**, 157401 (2004).
[36] T. Unold, K. Mueller, C. Lienau, T. Elsaesser, and A. D. Wieck, Phys. Rev. Lett. **94**, 137404 (2005).
[37] M. Wesseli, C. Ruppert, S. Trumm, H. J. Krenner, J. J. Finley, and M. Betz, Appl. Phys. Lett. **88**, 203110 (2006).
[38] B. Patton, W. Langbein, U. Woggon, L. Maingault, and H. Mari-

ette, Phys. Rev. B **73**, 235354 (2006).
[39] S. Sanguinetti, E. Poliani, M. Bonfanti, M. Guzzi, E. Grilli, M. Gurioli, and N. Koguchi, Phys. Rev. B **73**, 125342 (2006).
[40] B. Krummheuer, V. M. Axt, and T. Kuhn, Phys. Rev. B **65**, 195313 (2002).
[41] T. Takagahara, Phys. Rev. B **60**, 2638 (1999).
[42] A. Vagov, V. M. Axt, T. Kuhn, W. Langbein, P. Borri, and U. Woggon, Phys. Rev. B **70**, 201305(R) (2004).
[43] J. Förstner, C. Weber, J. Danckwerts, and A. Knorr, Phys. Rev. Lett. **91**, 127401 (2003).
[44] A. Krügel, V. M. Axt, and T. Kuhn, Phys. Rev. B **73**, 035302 (2006).
[45] P. Machnikowski and L. Jacak, Phys. Rev. B **69**, 193302 (2004).
[46] A. Vagov, V. M. Axt, and T. Kuhn, Phys. Rev. B **67**, 115338 (2003).
[47] W. Langbein, P. Borri, U. Woggon, V. Stavarache, D. Reuter, and A. D. Wieck, Phys. Rev. B **69**, 161301(R) (2004).
[48] V. M. Axt, T. Kuhn, A. Vagov, and F. M. Peeters, Phys. Rev. B **72**, 125309 (2005).
[49] Y. Z. Hu, S. W. Koch, M. Lindberg, N. Peyghambarian, E. L. Pollock, and F. F. Abraham, Phys. Rev. Lett. **64**, 1805 (1990).
[50] T. Takagahara, Phys. Rev. B **39**, 10206 (1989).
[51] P. Borri, W. Langbein, S. Schneider, U. Woggon, R. L. Sellin, D. Ouyang, and D. Bimberg, Phys. Status Solidi B **233**, 391 (2002).
[52] O. Benson, C. Santori, M. Pelton, and Y. Yamamoto, Phys. Rev. Lett. **84**, 2513 (2000).
[53] O. Gywat, G. Burkard, and D. Loss, Phys. Rev. B **65**, 205329 (2002).
[54] U. Hohenester, Phys. Rev. B **66**, 245323 (2002).
[55] X. Q. Li, Y. W. Wu, D. Steel, D. Gammon, T. H. Stievater, D. S. Katzer, D. Park, C. Piermarocchi, and L. J. Sham, Science **301**, 809 (2003).
[56] G. Mahan, *Many-Particle Physics* (Plenum, New York, 1990).
[57] B. Krummheuer, V. M. Axt, T. Kuhn, I. D'Amico, and F. Rossi, Phys. Rev. B **71**, 235329 (2005).
[58] L. Jacak, J. Krasnyj, D. Jacak, and P. Machnikowski, Phys. Rev. B **65**, 113305 (2002).
[59] E. A. Muljarov and R. Zimmermann, Phys. Rev. Lett. **93**, 237401 (2004).
[60] E. A. Muljarov, T. Takagahara, and R. Zimmermann, Phys. Rev. Lett. **95**, 177405 (2005).
[61] A. Vagov, V. M. Axt, and T. Kuhn, Phys. Rev. B **66**, 165312 (2002).
[62] S. T. Cundiff, M. Koch, W. H. Knox, J. Shah, and W. Stolz, Phys. Rev. Lett. **77**, 1107 (1996).
[63] B. Fluegel, N. Peyghambarian, G. Olbright, M. Lindberg, S. W. Koch, M. Joffre, D. Hulin, A. Migus, and A. Antonetti, Phys. Rev. Lett. **59**, 2588 (1987).
[64] M. Lindberg and S. W. Koch, Phys. Rev. B **38**, 7607 (1988).
[65] U. Neukirch, S. R. Bolton, L. J. Sham, and D. S. Chemla, Phys. Rev. B **61**, R7835 (2000).
[66] G. Bester, S. Nair, and A. Zunger, Phys. Rev. B **67**, 161306(R) (2003).
[67] W. Langbein and B. Patton, Phys. Rev. Lett. **95**, 017403 (2005).
[68] A. Krügel, V. M. Axt, T. Kuhn, A. Vagov, and F. Peeters, Phys. Status Solidi B **243**, 2241 (2006).